Diffusion Path Analysis of Dynamic Behavior of Oil-Water-Surfactant Systems

The diffusional processes that occur when oil contacts an aqueous surfactant solution have been investigated. These are pertinent to enhanced oil recovery by surfactant flooding and to detergency in certain systems. The theory of diffusion paths was used to solve the diffusion equations for a model pseudoternary system. Although detailed comparison with experimental results was not possible due to a lack of necessary data, calculated diffusion paths and interface velocities were found to be useful for explaining various phenomena observed experimentally in an oil recovery system.

Because the surfactant "solutions" studied commonly exist as dispersions of liquid crystal, extension of the theory to allow for initial compositions in two-phase regions was carried out. Also novel was investigation of the effect of the three-phase regions that occur in these systems on the position and shape of calculated diffusion paths.

K. H. Raney, C. A. Miller
Department of Chemical Engineering
Rice University
Houston, TX 77251

Introduction

When two liquid phases that are not in equilibrium are brought into contact, diffusion proceeds until equilibrium is attained. In surfactant systems these diffusional processes have been found to be particularly important in two practical applications. In enhanced oil recovery by chemical flooding, the dynamic behavior accompanying phase equilibration between the injected surfactant-brine mixture and the oil may well affect recovery efficiency (Lam et al., 1983; Chiang and Shah, 1981). Also, diffusion and phase transformation kinetics control the rate and manner of oily soil removal by solubilization and emulsification in detergency (Lawrence, 1959; Stevenson, 1961; Raney et al., 1987). As a result, nonequilibrium conditions have been studied in our laboratory for surfactant systems of interest in both applications (Raney et al., 1985; Benton et al., 1986).

A previous paper described in detail experimental observations of diffusion phenomena in two petroleum sulfonate systems typical of those used for enhanced oil recovery (Raney et al., 1985). A novel technique using videomicroscopy was found to allow detailed viewing of intermediate phase growth, interface motion, and spontaneous emulsification. Correlation of the results with equilibrium phase behavior was made as a function of system salinity, with differing phenomena occurring in the low-, intermediate-, and high-salinity regimes.

Here we describe an analytical diffusion path method that can be used to interpret many of these nonequilibrium phenomena. The method was applied to a model system simulating the phase behavior as a function of salinity of a typical oil-water-surfactant system found in oil recovery. Extension of the analysis to allow for initial mixtures that are stable dispersions was necessary because of the common occurrence of injected solutions that are liquid crystal dispersions (Benton and Miller, 1983).

Diffusion Path Analysis

Conventional theory

The use of diffusion paths is one way in which the diffusion processes between two phases can be described. It allows intermediate compositions and interfaces to be plotted in equilibrium phase space as an invariant path between the two initial compositions. Although diffusion path theory has most widely been used in metallurgy and ceramics (Kirkaldy and Brown, 1963; Christensen, 1977a), its applicability to liquid systems has also been demonstrated (Ruschak and Miller, 1972; Benton, et al., 1982).

The initial phases are modeled as being semiinfinite in extent. Although end effects may ultimately play a role in both oil recovery and detergency as the oil phase is consumed, the present theory, applicable in the initial stages of contacting, gives the basic behavior to be expected. Moreover, in our video microscopy experiments, which this paper aims to explain, both phases were of sufficiently large volume that end effects were negligible.

Transport by convection is neglected. Also, the overall mass density is assumed to be constant throughout the system. Once again, this assumption is not strictly correct in any actual contacting process. Severe deviations from theory can occur in liquid systems when intermediate phases form that are either more dense than the phase below or less dense than the phase above. This behavior produces large-scale natural convection within the system (Raney et al., 1985).

Diffusion coefficients are assumed to be constant in each phase, and cross-diffusion effects are assumed to be negligible. The theory has been modified to allow for cross-diffusion terms (Christensen, 1977b), but this complicates the mathematics significantly. In addition, there is a lack of data describing both cross-diffusion and concentration-dependent diffusion in most systems. Therefore, modification of these assumptions is of limited value at present.

An important assumption is that the moving planar interfaces are at equilibrium. This assumption requires that diffusion through the bulk phases be slow in comparison to adsorption and desorption at the interfaces. After a short initial period during which concentration gradients are large, it is probably valid. An exception is when an ordered phase, such as a liquid crystal, forms at an interface. Then phase transformation rates may be limited by nonequilibrium effects at the interface. Examples of such behavior have been reported for a nonionic and an anionic surfactant system by Friberg, Neogi, and coworkers (Friberg et al. 1985, 1986; Neogi et al., 1985).

Detailed solutions based on these assumptions may be found elsewhere (Ruschak and Miller, 1972; Danckwerts, 1950). For a ternary system, one-dimensional diffusion equations are written for each initial phase and any intermediate phases that form for the two independent diffusing species. As is well known, the boundary conditions with semiinfinite phases lead to error function solutions for the concentration profiles in terms of the similarity variable $\eta = x/(2\sqrt{Dt})$.

Actual interface compositions for a system with given phase behavior and known relative diffusion constants are found by solving component mass balances at each interface. The interface K values (the values of η at the interfaces) can be shown to be contants. Thus, the concentrations at each interface are invariant with time.

For an m-component system with n interfaces, $nm - n$ equations must be solved. The corresponding $nm - n$ unknowns are one K value at each interface and enough interfacial concentrations to specify a tie line. For a ternary system, one concentration at each interface is sufficient. In this study, these coupled, nonlinear equations were solved by a Newton-Raphson iteration technique.

Much important information can be obtained from diffusion path analysis. It allows prediction of spontaneous emulsification resulting from diffusion (Ruschak and Miller, 1972). In addition, the theory indicates that interface velocities obey the following relationship:

$$\frac{d\epsilon}{dt} = K\sqrt{\frac{D}{t}} \tag{1}$$

By defining each interface K value with a common diffusion constant, one can easily compare the calculated relative velocities of the various interfaces. Equation 1 also shows that interface position ϵ is directly proportional to $\sqrt{t}$. This property allows one to check whether diffusion path theory is consistent with an actual contacting experiment.

Extension for multiphase structures

In most studies of diffusion couples, single-phase initial compositions are used. Interfaces that form are usually planar and separate two single-phase materials. However, multiphase initial compositions and interfaces are sometimes encountered. Because conventional diffusion path theory does not account for these occurrences, extension of the theory has been made for application to oil-water-surfactant systems.

Two scales of resolution could be considered:

1. A fine scale where the shape and sizes of single-phase areas are distinguishable
2. A coarse scale that obscures most multiphase details

For this study, a coarse scale will be used in which local equilibrium is assumed everywhere and lateral diffusion is very rapid.

Another assumption is that diffusion occurs only on a molecular level; that is, particles of the dispersed phase are too large to diffuse. Molecular diffusion coefficients are assumed constant in each phase. Because diffusion occurs through channels of variable shape and cross section, the diffusion constants are multiplied by tortuosity factors that are functions of phase volume fraction.

Specifically, the derivations will be for a ternary diffusion couple with one of the initial compositions having two-phase structure, as shown in Figure 1. The objective is to calculate the diffusion path in this region starting at an overall initial composition w_{10}, w_{20}. Straight-line phase boundaries are assumed so as to simplify the equations.

For the general case of bicontinuous diffusion, Fick's law equations for components 1 and 2 are

$$\frac{\partial w_i}{\partial t} = D_i^* \frac{\partial}{\partial x}\left(Af\frac{\partial w_i^*}{\partial x}\right) + D_i^{**}\frac{\partial}{\partial x}\left(B(1-f)\frac{\partial w_i^{**}}{\partial x}\right) \qquad i = 1, 2 \tag{2}$$

where A and B are tortuosity factors and f is the phase fraction of the single-starred phase. If w_1^* is known, the corresponding tie line specifies all other equilibrium compositions. Therefore, the Eqs. 2 can be rewritten in the following manner as similarity transformations of the normalized concentration $E = [w_1^* - w_1^*(\epsilon)]/[w_{10}^* - w_1^*(\epsilon)]$:

$$E'' = \frac{-2\eta\left\{\dfrac{(w_i^* - w_i^{**})\dfrac{dw_1^*}{dw_i^*}}{[w_{10}^* - w_1(\epsilon)]}f' + fE' + (1-f)\dfrac{dw_i^{**}}{dw_i^*}E'\right\} - \dfrac{D_i^*}{D_1^*}Mf'E' + \dfrac{D_i^{**}}{D_1^*}\dfrac{dw_i^{**}}{dw_i^*}Nf'E'}{\left[\dfrac{D_i^*}{D_1^*}Af + \dfrac{D_i^{**}}{D_1^*}\dfrac{dw_i^{**}}{dw_i^*}B(1-f)\right]} \qquad i = 1, 2 \tag{3}$$

In these equations, $\eta = x/(2\sqrt{D_1^* t})$ and a prime denotes differ-

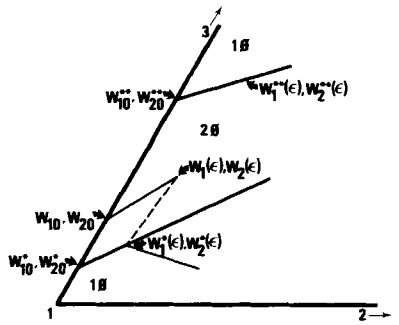

Figure 1. Phase diagram of diffusion path in a two-phase region.

entiation with respect to η. Also, $M = (dA/df)f + A$ and $N = (dB/df)(f-1) + B$.

Equations 3 cannot be decoupled to get analytical expressions for f in terms of E. Instead, solving for f' by eliminating E'' between the equations yields

$$f' = \frac{E'\left\{J\left[(1-f)\dfrac{dw_1^{**}}{dw_1^*} + f\right] - L\left[(1-f)\dfrac{dw_2^{**}}{dw_2^*} + f\right]\right\}}{L\dfrac{(w_2^* - w_2^{**})}{[w_{10}^* - w_1^*(\epsilon)]}\dfrac{dw_1^*}{dw_2^*} - J\dfrac{(w_1^* - w_1^{**})}{[w_{10}^* - w_1^*(\epsilon)]} + \dfrac{E'}{2\eta}\left(LM\dfrac{D_2^*}{D_1^*} - LN\dfrac{D_2^{**}}{D_1^*}\dfrac{dw_2^{**}}{dw_2} - JM + JN\dfrac{D_1^{**}}{D_1^*}\dfrac{dw_1^{**}}{dw_1^*}\right)} \tag{4}$$

where

$$J = \frac{D_2^*}{D_1^*}Af + \frac{D_2^{**}}{D_1^*}\frac{dw_2^{**}}{dw_2^*}B(1-f)$$

and

$$L = Af + \frac{D_1^{**}}{D_1^*}\frac{dw_1^{**}}{dw_1^*}B(1-f)$$

The boundary conditions for Eqs. 3 and 4 are given as follows:

$$E\left(\eta = \frac{\epsilon}{2\sqrt{D_1^* t}} = K\right) = 0$$

$$E(\eta = \infty) = 1$$

$$f(\eta = \infty) = \frac{w_{10} - w_{10}^{**}}{w_{10}^* - w_{10}^{**}}$$

For assumed values of K and $w_1^*(\epsilon)$, a shooting method is used to determine the diffusion path, as shown in Figure 2. An initial guess of E' is made at η^* (a large value of η simulating infinity), allowing E'' and f' to be calculated at that point using Eqs. 3 and 4. The derivative terms allow calculation by finite differences of f, E, and E' at $\eta - \Delta\eta$. The process is repeated until $\eta = K$ is reached. If E is not approximately 0 to within a specified tolerance, the profile slope at η^* is adjusted, and the profile is

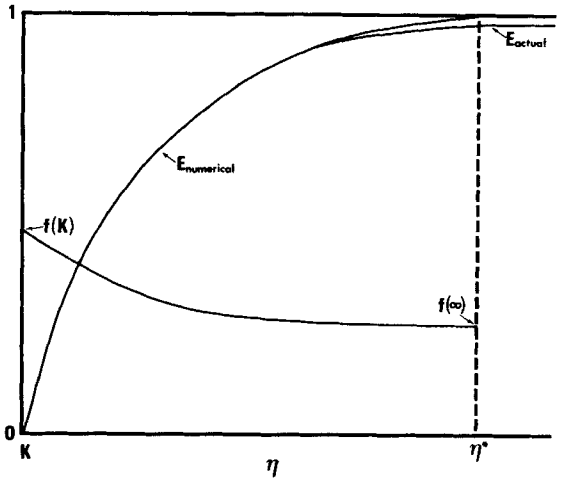

Figure 2. Diagram of numerical method used to determine phase fraction and normalized concentration profiles for a two-phase diffusion path.

recalculated. As would be expected, profiles have been found to be insensitive to the choice of η^* as long as the magnitude of the slope at that point is small. Mass fluxes at the interface, important when finding the complete diffusion path, can be determined numerically from the calculated profile and the phase fraction at the interface. If a mass balance is not attained at each interface along the diffusion path, the entire process must be repeated with new values of K and $w_1^*(\epsilon)$.

The analysis is simplified greatly when diffusion occurs in only one phase. For example, the diffusion equations, Eqs. 3, yield the following relationship when the tortuosity factor B is set equal to zero (the double-starred phase becomes dispersed):

$$\frac{dw_2}{dw_1} = \frac{D_2^*}{D_1^*}\left(\frac{dw_2^*}{dw_1^*}\right) = \text{constant} \tag{5}$$

In this case the diffusion path is a straight line on the ternary phase diagram that is independent of the shape of the dispersed-phase boundary and the rest of the diffusion path. When D_2^* equals D_1^*, the diffusion path parallels the boundary of the continuous phase. However, although the shape of the diffusion path is immediately known in this case, a numerical solution is still required to determine the concentration gradients at the interface.

The previous analysis assumes that a boundary forms at which one phase abruptly disappears. If the disappearing phase is dispersed in the other, the boundary will appear in the form of a dissolution front. This situation is analogous to that of fog vaporization (Toor, 1971). An interface between immiscible phases will form otherwise. These complex phase boundaries have been found to be compositionally invariant with η in ceramic systems, and therefore to be in accordance with coarse-scale diffusion path analysis (Christensen and Jepsen, 1971).

Phase Behavior Modeling

System representation

Typically, the phase behavior of surfactant systems for enhanced oil recovery is represented by a *pseudoternary* dia-

gram in which the vertices represent polar, nonpolar, and amphiphilic components. This two-dimensional representation has been used extensively in chemical flooding simulators because it allows for simple mathematical modeling of phase behavior (Pope and Nelson, 1978). For the same reason, a pseudoternary representation was used in this study with brine, oil, and a surfactant-alcohol mixture being chosen as the pseudocomponents.

Microemulsion regime

Figure 3 shows the typical progression of phase diagrams as salinity is increased in an anionic surfactant system (Healy et al., 1976; Bennett et al., 1981). At low salinities the surfactant mixture is preferentially water-soluble, forming an oil-in-water microemulsion. Increasing salinity results in the formation of a three-phase region at the lower critical endpoint. At the so-called optimal salinity, the middle-phase microemulsion solubilizes equal volumes of brine and oil. Eventually, a water-in-oil microemulsion forms at an upper critical end point as the surfactant becomes preferentially oil-soluble.

For our model system, phase behavior is based on a dimensionless salinity S. The lower critical end point, optimum salinity, and upper critical end point correspond to S values of 0, 0.5, and 1, respectively. The middle-phase vertex of the three-phase triangle is modeled as moving along a symmetric parabola from one critical end point to the other, the apex corresponding to optimal conditions (Pope and Nelson, 1978; Bennett et al., 1981). The excess brine and oil vertices move linearly on the ternary diagram between the critical end points. In this study, the surfactant pseudocomponent weight fraction was chosen to be 0.10 in the middle-phase microemulsion at optimal salinity and approximately 0.02 at the critical end points. The surfactant-alcohol concentration in the excess phases at optimal was assumed to be 0.125 wt. %.

The two-phase lobes are mathematically represented by a modified Hand model (Bennett et al., 1981; Hand, 1930). Symmetry is assumed with respect to dimensionless salinity, i.e., the diagrams at S and $1 - S$ are mirror images of one another. Also, the binodal lobes are assumed to retain their shape as they shrink or enlarge. Finally, plait point positions on the binodals vary with salinity, although they remain relatively constant in the overall ternary diagram. Further details of the model phase behavior may be found elsewhere (Raney, 1985).

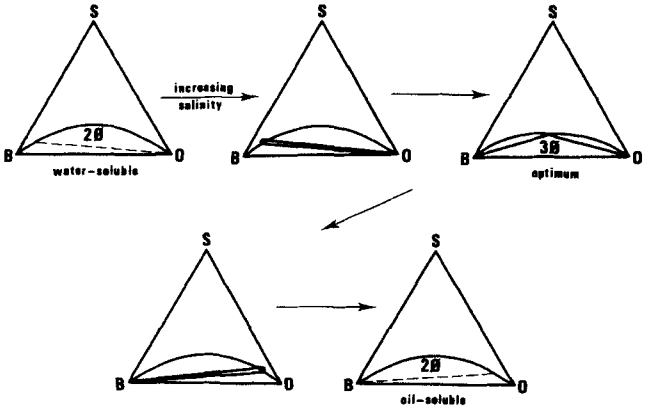

Figure 3. Progression of phase diagrams in an anionic surfactant system.

Liquid crystal regime

Little work has been done on modeling the pseudoternary phase behavior in the liquid crystal regime of oil-water-surfactant systems. This deficiency is due to a lack of data on the transition from aqueous liquid crystalline phases to microemulsions when oil is added, although some work along these lines has been reported (Ghosh and Miller, 1984).

A simple model is proposed that is based on the observation that many injection fluids for oil recovery are in the form of lamellar liquid crystal dispersions (Miller et al., 1982). Such dispersions can be described in terms of Figure 1. Brine, oil, and the surfactant-cosurfactant mixture are represented by components 1, 2, and 3, respectively. The region is modeled as two phases, a surfactant-rich liquid crystalline phase (top) and an isotropic phase containing predominantly brine.

The two phase boundaries are modeled as straight lines. As mentioned previously, this assumption simplifies the mathematics when diffusion paths within the two-phase region are calculated. Also, it has little adverse effect when diffusion paths extend only a small distance into the two-phase region, a common occurrence in our calculations.

The positions and slopes of the phase boundaries are functions of the dimensionless salinity S. Due to the decrease in ionic surfactant solubility in brine, the phase boundaries move toward the brine corner as system salinity is increased, thereby increasing the fraction of liquid crystal for a given initial composition. For this study, all diffusion paths were calculated for an initial aqueous system containing 10 wt. % surfactant. The lower phase boundary intercepted the brine-surfactant axis at surfactant concentrations typical of critical micelle concentrations (from approximately 0.25 to 0.05 wt. % surfactant). The liquid crystal boundary position was chosen such that the initial aqueous system was a liquid crystal dispersion at low salinities, contained about 50% liquid crystal at the lower critical end point, and became entirely liquid crystal at the upper critical end point. This behavior resembles that found in the systems studied experimentally (Raney et al., 1985).

Equilibrium tie lines are modeled based on the relative fraction of oil in the two phases. In the simplest case, the one chosen for this study, the tie lines are parallel to the brine-surfactant axis, indicating equal partitioning of oil between the liquid crystal and the isotropic phase. A diffusion path crossing tie lines oriented in this manner is shown in Figure 1.

Diffusion properties

In addition to equilibrium phase behavior, diffusion path analysis requires the relative values of diffusion constants in each phase crossed by the diffusion path. For oil-water-surfactant systems, complete diffusion data are not available. In fact, most measurements have been limited to self-diffusion studies of microemulsions (Lindman et al., 1980, 1981). Although useful for characterizing phase structure, self-diffusion coefficients are not strictly applicable to diffusional processes that result from concentration gradients.

As a result of this limitation on diffusion data, equal diffusion constants in all phases were assumed in this study. In addition, cross-diffusion effects were neglected. These assumptions, which have proved adequate for diffusion path analyses of oil-water-alcohol systems (Ruschak and Miller, 1972), result in straight path segments within each phase region crossed on the ternary phase diagram.

Modeling diffusion in the two-phase region requires tortuosity factors for both the liquid crystal and isotropic phases. These values are assumed to be functions of phase fraction only. This assumption is based on studies of diffusion in porous media, which have found that tortuosity factors depend only on porosity for a fixed medium geometry (Currie, 1965).

In this study, tortuosity factors corresponding to three-dimensional, simple cubic lattice site percolation were used (Kirkpatrick, 1973; Raney, 1985). This model has a percolation threshold of $\phi = 0.307$. Therefore, at liquid crystal fractions below this value diffusion is assumed to take place entirely in the isotropic phase. By symmetry, diffusion does not take place in the isotropic phase at liquid crystal fractions greater than $1 - \phi = 0.693$. Bicontinuous diffusion occurs at intermediate liquid crystal fractions.

Calculated Diffusion Paths

A summary of diffusion path results for the model system described in the previous sections is given in Figure 4. In this diagram the intermediate phases and calculated interface K values are shown as a function of dimensionless salinity S. As discussed in the theory section, interface K values are dimensionless quantities that give the interfacial positions at any given time. Here, because all of the values are based on a single diffusion constant, they are also proportional to the relative velocities of the interfaces. A positive value in Figure 4 indicates upward movement of an interface.

Also shown are experimental points from the results of a previous investigation (Raney et al., 1985). Key features of the model system phase behavior described above were based on the oil-water-surfactant system used in that study. Also, knowledge obtained from the contacting experiments was found to be a valuable aid in the search for valid diffusion paths. A description of the experimental data is given in a later section where the model and experimental results are compared. First, descriptions of calculated diffusion paths in the three salinity regimes separated by the vertical dashed lines in Figure 4 are given.

Low salinities

The phase diagram in Figure 5 represents phase behavior at a typical salinity below the lower critical end point. The initial compositions of the aqueous and oleic phases are D and O, respectively. As is evident from the diagram, the initial phase fraction of liquid crystal is approximately 0.2, well below the percolation threshold of 0.307 where the liquid crystal phase becomes continuous.

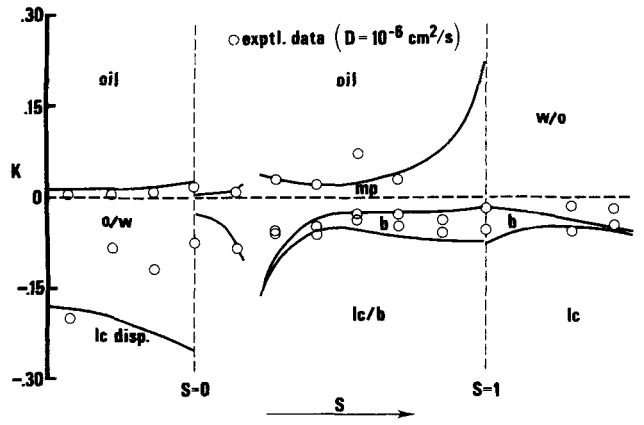

Figure 4. Model and experimental interface K values.
o/w, oil-in-water microemulsion; lc, liquid crystal; mp, middle-phase microemulsion; b, brine; w/o, water-in-oil microemulsion.

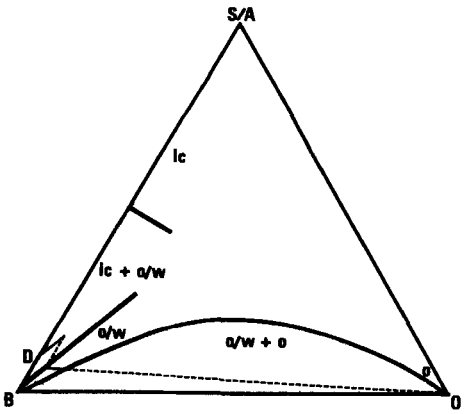

Figure 5. Calculated low-salinity diffusion path.

The only solutions found in this region were those where an intermediate oil-in-water microemulsion formed between the initial liquid crystal dispersion and the oil. These solutions predict the existence of a moving front where liquid crystal dissolves and where the composition of the aqueous phase is continuous. As indicated by Figure 4, the intermediate microemulsion phase grows much more rapidly downward than upward toward the oil. The low rate of oil solubilization is expected since the brine-continuous microemulsion contains only a small amount of oil for these conditions.

Intermediate salinities

As salinity is increased to the lower critical endpoint ($S = 0$), little change occurs in the calculated diffusion paths and interface velocities despite the initiation of bicontinuous diffusion in the aqueous region due to an increasing starting fraction of liquid crystal. Above the critical end point, however, complex phase behavior on the aqueous side of the ternary phase diagram causes a deviation in the sequence of diffusion paths.

Phase behavior studies (Ghosh and Miller, 1984) have shown that at salinities just above the lower critical end point, the liquid crystal-brine and brine-microemulsion two-phase regions interact to form a three-phase region, which is shown in Figure 6. A path below this new three-phase region and through the brine

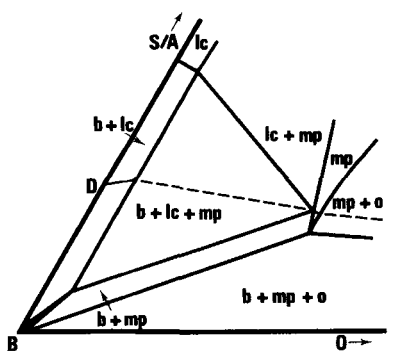

Figure 6. Calculated diffusion path at $S = 0.17$.

phase is not possible until well into the middle-phase regime at $S = 0.22$. Up to that salinity, calculations for this type of diffusion path predict a physically unrealistic situation with the brine-microemulsion interface moving faster than and in the same direction as the liquid crystal boundary ahead of it.

As an alternative, diffusion paths were calculated that form a complex interface across the three-phase triangle. Interfaces such as this have been predicted and observed in metal and ceramic systems (Christensen, 1977a; Rhines, 1956). Figure 6 shows the calculated path for $S = 0.17$. Although this path, which exits the three-phase region at the microemulsion vertex, is the only one possible for the given phase behavior, passage out on the adjoining sides of the triangle would also be allowable for other phase geometries. In those cases, spontaneous emulsification of liquid crystal or brine in the microemulsion would be predicted. The interface K values for diffusion paths across the three-phase region are shown at salinities just above the lower critical end point in the overall salinity scan presented in Figure 4.

The discontinuity in K values near $S = 0$ cannot be attributed to the critical end point phenomenon since paths like that of Figure 5 do exist at and very slightly above $S = 0$. Instead, the sudden change in behavior stems from formation of the three-phase region containing liquid crystal, which precludes further paths similar to Figure 5. Since no attempt has been made to model the details by which this region develops, the calculated K values exhibit a discontinuity at $S = 0$.

Diffusion paths were also calculated in this regime that pass through the liquid crystal phase, an example of which is shown in Figure 7 for $S = 0.10$. These calculations show growth of a middle-phase microemulsion in both directions. However, instead of the initial liquid crystal-brine mixture converting directly into a microemulsion, as at low salinities or as indicated by the diffusion paths crossing the three-phase triangle, a thin liquid crystal layer is predicted to form and grow between them. A calculated diffusion path with an interface across the three-phase region is also shown in Figure 7, illustrating the possibility of multiple diffusion paths in a system with given phase behavior and diffusion constants.

Figure 8 is an expanded plot of the calculated interface K values in the salinity regime around the lower critical end point ($S = 0$). It shows that passage through the liquid crystal layer is only possible up to $S = 0.13$ with the assumed phase behavior. Therefore, for a salinity range from $S = 0.13$ to $S = 0.22$, passage above or below the three-phase region is not feasible. Paths across the three-phase triangle were found from the lower critical end point to $S = 0.17$. Above this value of S paths of this type were constrained by the model phase behavior to lie entirely above the straight line between the end compositions, thereby preventing attainment of an overall mass balance. As a result, for phase diagrams like those shown in Figures 6 and 7, no solution above, below, or across the three-phase triangle could be determined between $S = 0.17$ and $S = 0.22$. However, the precise locations of the various phase boundaries were somewhat arbitrary in this region, and small changes permitted diffusion paths crossing the three-phase triangle to exist over the entire salinity range up to $S = 0.22$. Nevertheless, this study shows that a rigorous diffusion path cannot always be found for a well-characterized system.

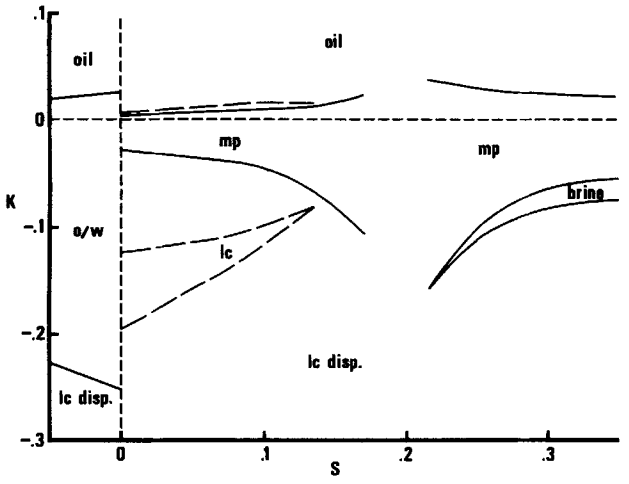

Figure 8. Model interface K values at salinities near the lower critical endpoint.

At $S = 0.22$ the middle-phase microemulsion becomes sufficiently oil-rich that a brine layer can begin forming below it. With increasing salinity, the brine, which is an equilibrium phase along with the microemulsion, forms faster. In this intermediate salinity regime, which is most desirable for enhanced oil recovery, the calculated diffusion paths lie close to the large three-phase triangle, as shown in Figure 9 for $S = 0.50$, indicating only small composition changes within the phases. Note that the analysis predicts a very short diffusion path segment

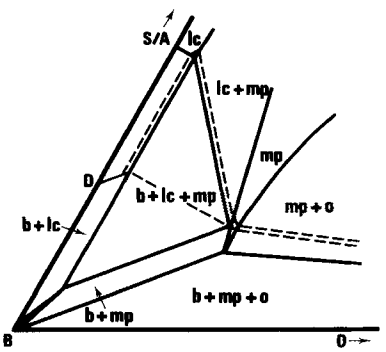

Figure 7. Calculated diffusion paths at $S = 0.10$.

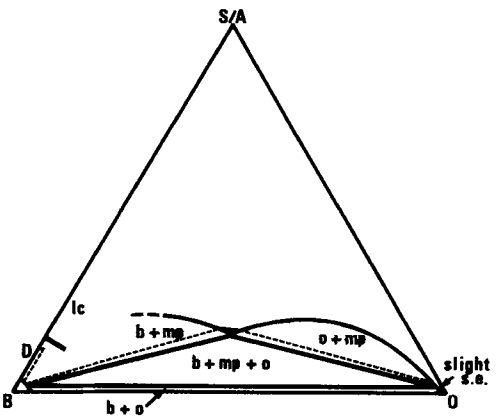

Figure 9. Diffusion path at optimal salinity indicating slight spontaneous emulsification of brine in the oil phase.

between point D and the front where liquid crystal dissolves. Although both brine and liquid crystal exist throughout this region, the liquid crystal is present in greater quantity and is the continuous phase. In contrast, brine is the continuous phase for the low-salinity situation of Figure 5.

High salinities

The transition that occurs in diffusion paths near the upper critical end point is not as complex as that at the low-salinity end. As the three-phase region shrinks into the critical tie line, the diffusion path continues to pass through the middle-phase microemulsion. However, because the diffusion path tie line lies below the critical tie line at the critical end point, a switch in diffusion paths occurs at values of S very slightly below unity as the path begins passing under the three-phase triangle. A schematic illustration of this progression is shown in Figure 10. Spontaneous emulsification is shown to occur at these conditions above optimal salinity due to the oil-brine two-phase region being crossed by the oil segment of the diffusion path. This criterion for the prediction of spontaneous emulsification has previously been shown to be valid for oil-water-alcohol systems (Ruschak and Miller, 1972). Figure 4 indicates that the relative velocity of the oil-microemulsion interface increases rapidly as the compositions across the interface approach each other.

The path in Figure 11 is representative of those calculated for high salinities. A significant amount of spontaneous emulsification of brine is predicted to occur in the oil phase as it converts to a water-in-oil microemulsion. Note that the initial aqueous structure of the model system is entirely liquid crystalline for these conditions.

A summary of the number and type of calculated diffusion paths in the various salinity regimes is shown in Table 1.

Comparison to contacting experiments

Comparison of the model results over the entire salinity range can be made to microscopic contacting experiments performed at ambient conditions with an extensively studied orthoxylene sulfonate system (Healy et al., 1976). Detailed experimental observations are reported elsewhere (Raney et al., 1985). In that study, the small sample dimensions hindered convection and provided diffusion-controlled phase growth at all salinities for periods of up to one week. Accordingly, diffusion path theory should be applicable.

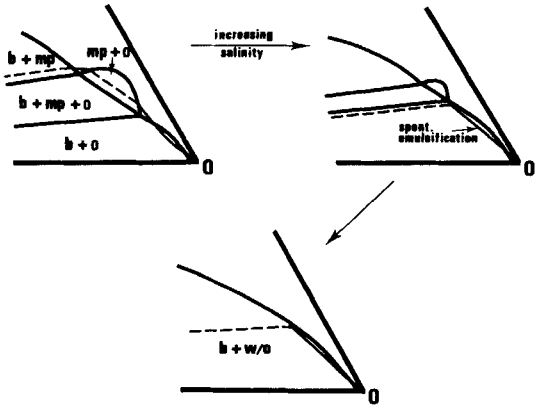

Figure 10. Transition in diffusion paths at upper critical end point.

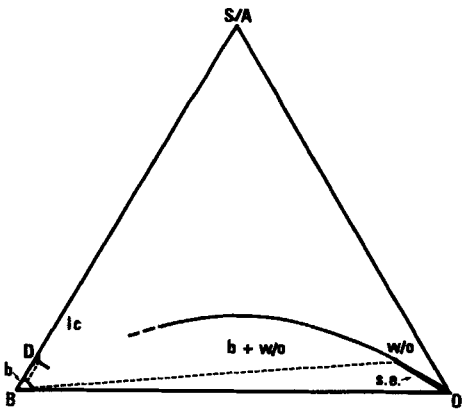

Figure 11. High-salinity diffusion path indicating extensive spontaneous emulsification in the oil phase.

Shown in Figure 4 with the model curves are experimental interface K values. These were determined from the measured slope of interface position vs. the square root of time using the following equation, which can be derived directly from Eq. 1:

$$K = \frac{d\epsilon/d\sqrt{t}}{2\sqrt{D}}$$

Here, D represents an effective overall diffusion constant for the system. A good match with K values for the calculated diffusion paths is found when D is taken to be 10^{-6} cm^2/s, not an unreasonable value for a surfactant system. For an effective constant of 10^{-5} cm^2/s, a value more typical for surfactant-free systems, the magnitudes of the experimental K values would be three times smaller than those shown in Figure 4 and significantly less than the model results. Inherent in these comparisons is the assumption that the model pseudoternary phase behavior char-

Table 1. Calculated Diffusion Paths for Model Salinity Scan

Dimensionless Salinity	No. of Path Types	Description
$S \le 0.$	1	Oil-in-water microemulsion between liquid crystal dispersion and oil
$0 < S \le 0.13$	2	(a) Middle-phase microemulsion between liquid crystal-brine mixture and oil (b) Liquid crystal and middle-phase microemulsion between liquid crystal-brine mixture and oil
$0.13 < S \le .17$	1	Middle-phase microemulsion between liquid crystal-brine mixture and oil
$0.17 < S < 0.22$	0	None
$0.22 \le S < 1$	1	Brine and middle-phase microemulsion between liquid crystal-brine mixture and oil
$1 \le S$	1	Brine between liquid crystal and water-in-oil microemulsion

acterizes with sufficient accuracy the phase behavior of the experimental system.

Apparently, the rate of the entire diffusion process is controlled by transport within a phase (or phases) exhibiting inhibited diffusion as compared to typical liquid mixtures of small molecules. In the system of interest here, the "limiting" phase could be either liquid crystal or microemulsion, both of which are present at all salinities and which, due to their structure, have been shown to exhibit restricted diffusion properties (Lindman et al., 1980; Tiddy, 1980). For example, the microemulsions that form at both low and high salinities exist as a dispersion of drops in a continuous medium. As a result, the transport of the dispersed phase, e.g., oil in an oil-in-water microemulsion, and the continuous phase can be characterized by a binary diffusion constant. Since the drops are roughly an order of magnitude larger than a solvent molecule, their effective diffusivity, based on the Stokes-Einstein relationship, would be expected to be an order of magnitude less than that for molecules in a structureless liquid. Therefore, as shown at both low and high salinities in Figure 4, the formation of an oil-in-water (or water-in-oil) microemulsion during a contacting experiment probably results in slower equilibration rates than would normally be expected for a typical liquid system. Of course, this representation of drop diffusion in a microemulsion is an oversimplification due to the continual exchange of molecules between individual drops and between drops and the continuous phase.

Qualitative agreement is found between the experiments and theory regarding which intermediate phases form at different salinities. At low salinities the liquid crystalline dispersion fronts and the intermediate microemulsion phases predicted by the calculations were observed experimentally. Just above the lower critical end point salinity in the contacting experiments, a middle-phase microemulsion began forming as an intermediate phase. A brine layer did not form, however, even though an excess brine phase would be expected at equilibrium. These observations can best be explained by diffusion paths like the one in Figure 6, which passes across the three-phase region. Although a buildup of dispersed liquid crystal was observed below the microemulsion in this salinity regime, a two-phase structure appeared to be maintained at the interface (Raney et al., 1985). If correct, this observation would rule out diffusion paths passing over the three-phase triangle and through the liquid crystalline phase, Figure 7. However, additional experiments with improved microscope optics are needed to provide conclusive information on which path is actually operative at these salinities.

The occurrence of a microemulsion as the only intermediate phase was seen for values of S below about 0.22. As indicated previously, it is possible to find diffusion paths similar to that of Figure 6 for S in this range if the compositions of the microemulsion in equilibrium with liquid crystal and brine are modified slightly from those assumed in the calculations leading to Figure 4. When S exceeded about 0.22, a permanent brine layer appeared as a second intermediate phase in the contacting experiments, as predicted by the diffusion path analysis for the model system. Also, both the predicted increasing growth rate of the brine phase and the enhanced solubilization of oil by the microemulsion were observed experimentally as salinity was increased past its optimal value. Finally, spontaneous emulsification of brine drops in the oil phase was found to occur above optimal salinity, the point at which it was predicted to initiate by diffusion path theory.

This study would seem to indicate that diffusion path analysis, even without accurate diffusion constant data, can qualitatively explain the nonequilibrium phenomena in a pseudoternary liquid system with complicated phase behavior. For this study, the use of a single effective diffusion constant in all phases provided not only an accurate prediction of the intermediate phases that would be present at a particular salinity, but also the relative rates at which those phases would form. Apparently these phenomena, as well as spontaneous emulsification, are much more dependent in these systems on equilibrium phase behavior than on the relative rates of diffusion of components in the various phases.

Both experimental and theoretical evidence was found indicating formation of an interface across a three-phase region at salinities just into the middle-phase microemulsion regime. The corresponding diffusion path is indicative of what can occur when passage either above or below a three-phase region is not possible. Because this system was constrained to have the initial aqueous composition in an adjacent two-phase region, further studies of the effect on diffusion paths of three-phase regions between two single-phase starting structures appear justified. Other topics worthy of further investigation are the existence of multiple diffusion paths or of no diffusion paths for certain diffusion couples, and the transition between two types of diffusion paths, e.g., the transition in paths shown in Figure 10.

Acknowledgment

This work was supported by grants from Shell Development Co., Exxon Production Research Co., Amoco Production Co. and Gulf Research and Development Co.

Notation

A = tortuosity factor for * phase
B = tortuosity factor for ** phase
D = diffusion constant
D_i^* = diffusion constant for component i in * phase
D_i^{**} = diffusion constant for component i in ** phase
E = normalized concentration along two-phase diffusion path
E' = first derivative of E with respect to η
E'' = second derivative of E with respect to η
f = phase fraction of * phase
f' = first derivative of f with respect to η
J = defined in Eq. 4
K = value of η at interface
L = defined in Eq. 4
M = defined in Eq. 3
N = defined in Eq. 3
S = salinity in model system
t = elapsed time after initial contact
w_i = overall weight fraction of component i
w_i^* = weight fraction of component i in * phase
w_i^{**} = weight fraction of component i in ** phase
x = translational position

Greek letters

ϵ = interface position
η = similarity variable
η^* = large value of η to simulate infinity
ϕ = percolation threshold

Literature Cited

Bennett, K. E., C. H. K. Phelps, H. T. Davis, and L. E. Scriven, "Microemulsion Phase Behavior—Observations, Thermodynamic Essentials, Mathematical Simulation," *Soc. Pet. Eng. J.*, **21**, 747 (1981).

Benton, W. J., and C. A. Miller, "Lyotropic Liquid Crystalline Phase and Dispersions in Dilute Anionic Surfactant-Alcohol-Brine Systems. 1: Patterns of Phase Behavior," *J. Phys. Chem.*, **87**, 4981 (1983).

Benton, W. J., C. A. Miller, and T. Fort, Jr., "Spontaneous Emulsification in Oil-Water-Surfactant Systems," *J. Disp. Sci. Technol.*, **3**, 1 (1982).

Benton, W. J., K. H. Raney, and C. A. Miller, "Enhanced Videomicroscopy of Phase Transitions and Diffusional Phenomena in Oil-Water-Nonionic Surfactant Systems," *J. Colloid Interface Sci.*, **110**, 363 (1986).

Chiang, M. Y., and D. O. Shah, "The Effect of Alcohol on Surfactant Mass Transfer across the Oil/Brine Interface and Related Phenomena," *Surface Phenomena in Enhanced Oil Recovery*, D. O. Shah, ed., Plenum, New York (1981).

Christensen, N. H., "Multiphase Ternary Diffusion Couples," *J. Am. Ceram. Soc.*, **60**, 293 (1977a).

———, "Ternary Diffusion with Two Moving Boundaries," *J. Am. Ceram. Soc.*, **60**, 54 (1977b).

Christensen, N. H., and O. L. Jepsen, "Diffusion in Three-Component Cement Clinkers," *J. Am. Ceram. Soc.*, **54**, 208 (1971).

Currie, J. A., "Gaseous Diffusion in Porous Media," *Br. J. Appl. Phys.*, **11**, 314 (1965).

Danckwerts, P. V., "Unsteady-State Diffusion or Heat Conduction with Moving Boundary," *Trans. Faraday Soc.*, **46**, 701 (1950).

Friberg, S. E., M. Mortensen, and P. Neogi, "Hydrocarbon Extraction into Surfactant Phase with Nonionic Surfactants. I: Influence of Phase Equilibria for Extraction Kinetics," *Sep. Sci. Technol.*, **20**, 285 (1985).

Friberg, S. E., M. Podzimek, and P. Neogi, "Transient Liquid Crystals in a W/O Microemulsion," *J. Disp. Sci. Technol.*, **7**, 57 (1986).

Ghosh, O., and C. A. Miller, "Phase Behavior at Low Oil Contents in Systems Containing Anionic Surfactants," *J. Colloid Interface Sci.*, **100**, 444 (1984).

Hand, D. B., "Dineric Distribution. I: The Distribution of a Consolute Liquid between Two Immiscible Liquids," *J. Phys. Chem.*, **34**, 1961 (1930).

Healy, R. N., R. L. Reed, and D. G. Stenmark, "Multiphase Microemulsion Systems," *Soc. Pet. Eng. J.*, **16**, 147 (1976).

Kirkaldy, J. S., and L. C. Brown, "Diffusion Behavior in Ternary Multiphase Systems," *Can. Met. Q.*, **2**, 89 (1963).

Kirkpatrick, S., "Percolation and Conduction," *Rev. Mod. Phys.*, **45**, 574 (1973).

Lam, A. C., R. S. Schechter, and W. H. Wade, "Mobilization of Residual Oil Under Equilibrium and Nonequilibrium Conditions," *Soc. Pet. Eng. J.*, **23**, 781 (1983).

Lawrence, A. S. C., "The Mechanism of Detergence," *Nature*, **183**, 1491 (1959).

Lindman, B., N. Kamenka, T. M. Kathopoulis, B. Brun, and P. G. Nilsson, "Translational Diffusion and Solution Structure of Microemulsions," *J. Phys. Chem.*, **24**, 2485 (1980).

Lindman, B., P. Stilbs, and M. E. Moseley, "Fourier Transform NMR Self-Diffusion and Microemulsion Structure," *J. Colloid Interface Sci.*, **83**, 569 (1981).

Miller, C. A., S. Mukherjee, W. J. Benton, J. Natoli, S. Qutubuddin, and T. Fort, Jr., "Liquid Crystals and Microemulsions in Oil Recovery," *AIChE Symp. Ser.*, **78**, 28 (1982).

Neogi, P., M. Kim, and S. E. Friberg, "Hydrocarbon Extraction into Surfactant Phase with Nonionic Surfactants. II: Model," *Sep. Sci. Technol.*, **20**, 613 (1985).

Pope, G. A., and R. C. Nelson, "A Chemical Flooding Compositional Simulator," *Soc. Pet. Eng. J.*, **18**, 339 (1978).

Raney, K. H., "Studies of Nonequilibrium Behavior in Surfactant Systems Using Videomicroscopy and Diffusion Path Analysis," Ph.D. Thesis, Rice Univ. Houston, TX (1985).

Raney, K. H., W. J. Benton, and C. A. Miller, "Use of Videomicroscopy in Diffusion Studies of Oil-Water-Surfactant Systems," *Macro- and Microemulsions*, D. O. Shah, ed., Am. Chem. Soc., Washington, DC (1985).

———, "Optimum Detergency Conditions with Nonionic Surfactants. I: Ternary Water-Surfactant-Hydrocarbon Systems," *J. Colloid Interface Sci.*, **117**, 282 (1987).

Rhines, F. K., *Phase Diagrams in Metallurgy*, McGraw-Hill, New York (1956).

Ruschak, K. J., and C. A. Miller, "Spontaneous Emulsification in Ternary Systems with Mass Transfer," *Ind. Eng. Chem. Fundam.*, **11**, 534 (1972).

Stevenson, D. G., "Ancillary Effects in Detergent Action," *Surface Activity and Detergency*, K. Durham, ed., Macmillan, London (1961).

Tiddy, G. J. T., "Surfactant-Water Liquid Crystal Phases," *Phys. Rep.*, **57**, 1 (1980).

Toor, H. L., "Fog Vaporization and Condensation in Boundary Value Problems," *Ind. Eng. Chem. Fundam.*, **10**, 121 (1971).

Manuscript received Nov. 13, 1986, and revision received Mar. 13, 1987.